Ueno, H. (1984) *Biochemistry 23*, 4791-4798.
Ueno, H., & Ooi, T. (1978) *J. Biochem. (Tokyo) 83*, 1423-1433.
Weber, A., & Murray, J. M. (1973) *J. Biol. Chem. 238*, 599-605.
Williams, D. L., Jr., & Swenson, C. A. (1981) *Biochemistry 20*, 3856-3864.
Woods, E. F. (1969) *Int. J. Protein Res. 1*, 29-45.
Wu, C.-S. C., & Yang, J. T. (1976) *Biochemistry 15*, 3007-3014.

Effect of Various Anions on the Stability of the Coiled Coil of Skeletal Muscle Myosin†

Walter F. Stafford, III*

Department of Muscle Research, Boston Biomedical Research Institute, and Department of Neurology, Harvard Medical School, Boston, Massachusetts 02114

Received April 16, 1984; Revised Manuscript Received December 31, 1984

ABSTRACT: The stability of skeletal myosin rod was studied by following the dependence of both papain digestion kinetics and helix–coil transition temperatures on the concentration of neutral salts. The rate of papain-catalyzed digestion of rod to form subfragment 2 and light meromyosin was strongly dependent on chloride concentration but essentially independent of acetate concentration up to 2.0 M. The rod exhibited a biphasic melting curve in 0.6 M NaCl, 5 mM phosphate, and 0.1 mM ethylenediaminetetraacetic acid (EDTA), pH 7.3, with transitions at 45 and 53 °C. In 0.6 M CH_3COONa, 5 mM phosphate, and 0.1 mM EDTA, pH 7.3, the transitions occurred at 50 and 58 °C, respectively. Transition temperatures were obtained with a novel curve-fitting method. The effect of increasing chloride ion concentration on melting profiles was 2-fold. Below 0.6 M salt, the two transition temperatures, $T_{m,1}$ and $T_{m,2}$, depended on salt concentration such that increasing NaCl concentration caused a small stabilization of the helix while increasing acetate concentration caused the helix to become markedly more stable. Between 0.6 and 1.0 M, variation of chloride concentration had almost no effect on the thermal stability of the rod while increasing acetate concentration increased its stability considerably. Above 1.0 M NaCl, the melting profiles became broad with a third transition being observed (e.g., at 3.0 M, $T_{m,3}$ = 38 °C), indicating the existence of a region which has a tendency to be destabilized by chloride. The third transition was not observed at comparable concentrations of acetate. This effect of chloride was not expected on the basis of its position in the Hofmeister series. Taken together, these observations suggested that while increasing salt concentration stabilizes the major portion of the coiled coil, chloride ion destabilizes a domain near the subfragment 2/light meromyosin junction with a concomitant increase in its susceptibility to proteolysis by papain.

Myosin consists of two high molecular weight polypeptides (heavy chains, M_r 200000) assembled into two morphologically distinct regions; it has a rod-shaped tail composed of two α-helical polypeptide chains wrapped in the coiled-coil configuration. At the N-terminus of each chain is a globular head which contains the ATPase and actin binding sites. Each myosin head, in turn, has bound to it two different low molecular weight subunits (light chains, M_r ~20000). Cleavage of myosin with various proteolytic enzymes produces distinct subfragments, each of which retains specific functions of the parent molecule (Lowey et al., 1969). The proteolytic susceptibility of two regions, one between the head and tail and the other between subfragment 2 and light meromyosin, has been taken to indicate flexibility in them. The flexibility of myosin and myosin rod has been investigated through a number of independent measurements of viscosity (Burke et al., 1973; de la Torre & Bloomfield, 1980), electrical birefringence (Highsmith et al., 1977), polarized light scattering (Highsmith et al., 1982), fluorescence depolarization (Harvey & Cheung, 1977), viscoelastic properties (Rosser et al., 1977; Hvidt et al., 1982; 1983), and electron microscopy (Elliott & Offer, 1978).

The effect of neutral salts on the stability of protein structure is well-known (Von Hippel & Scleich, 1969). Effects of salts on myosin ATPase activity and structure have been investigated (Warren et al., 1960; Brahms & Brezner, 1961; Tonomura et al., 1962; Seidel, 1969) and were found to follow the Hofmiester series (Hofmiester, 1888) for most ions studied. In a study by Stafford & Margossian (1982), the salt concentration dependence of the rate of papain-catalyzed proteolysis of myosin rod was found to depend on the type of anion according to the Hofmeister series (vis., citrate > sulfate > phosphate > acetate). It was observed subsequently that the concentration dependence of the rate constant in chloride, which was expected to be less than that of acetate, was out of order. This observation led to the investigation described below in which the effects of chloride on both the papain digestion kinetics and the thermal stability of myosin rod were studied.

Since chloride ion is used extensively to control ionic strength in in vitro experiments with myosin, it seemed worthwhile to

†This work was supported by National Institutes of Health Grant HL-26229.

* Address correspondence to this author at the Department of Muscle Research, Boston Biomedical Research Institute.

0006-2960/85/0424-3314$01.50/0

investigate the effect in some detail especially since the in vivo chloride ion concentration is in the millimolar range (Adrian, 1961; Harris, 1963; Bolton & Vaughan-Jones, 1977; Macchia & Baumgarten, 1979). Specific effects of chloride ion on the myosin coiled-coil structure have not been reported previously. An account of this work was presented at the San Antonio Meeting of the Biophysical Society (Stafford, 1984a) and the 1984 Meeting of the International Biophysics Congress in Bristol (Stafford, 1984b).

Experimental Procedures

Preparation of Myosin and Rod. Rabbit skeletal muscle myosin was prepared as described by Margossian & Lowey (1982). Skeletal myosin rod was prepared by papain digestion of insoluble myosin (Margossian et al., 1981). Myosin and rod preparations were stored in 50% glycerol at −24 °C.

Papain Digestion of Skeletal Myosin Rod. Digestion of rod by papain was carried out at 22 °C under various sets of ionic conditions essentially as described earlier (Kominz et al., 1965; Lowey et al., 1969; Stafford et al., 1979). Rod samples (15 g/L) were diluted into the appropriate buffers to a final concentration of 0.15–0.50 g/L. Aliquots were taken at various time intervals after papain addition (0.3 μM final concentration) and added to test tubes containing iodoacetic acid (IAA)[1] (5 mM final concentration). These samples were allowed to react with IAA at room temperature for 5 min and then kept at 0 °C until the time series was completed. Sodium dodecyl sulfate (1% final concentration) and dithiothreitol (10 mM final concentration) were added and the samples heated for 1 min at 100 °C and then dialyzed for 1–2 h against running buffer. Bromophenol blue (0.02% final concentration), dithiothreitol (10 mM final concentration), and glycerol (2% final concentration) were added and the samples kept frozen overnight at −24 °C. Electrophoresis was carried out on 8% microslab polyacrylamide gels (Matsudaira & Burgess, 1978) run at 100 V for 1.5 h and stained for 30 min 0.02% Coomassie brilliant blue R-250. For quantitative analysis of digestion kinetics, 5% cylindrical polyacrylamide gels (0.6 × 6 cm) were run as described by Stafford & Yphantis (1972) using a Tris–dodecyl sulfate/Tris–acetate, pH 8.1, buffer system. Gels were run at 100 V for 3 h, stained overnight in 0.01% Coomassie brilliant blue R-250 in 10% methanol and 10% acetic acid, and destained in the same solvent.

The effect of variations in salt concentration on the reactivity of papain was examined by following the hydrolysis of benzoyl-L-arginine ethyl ester (BAEE) at 255 nm in the same buffers as used for the digestion with 0.3 μM papain and 50 μM BAEE. At a given salt concentration, there was no difference in rate depending on whether acetate or chloride was present. Although it is unclear whether or not one is justified in using the esterase activity as a control for peptidase activity, this control at least showed that high concentrations of acetate did not denature the enzyme.

Circular Dichroism and Optical Rotation Measurements. Melting curves of myosin rod were obtained by following either the optical rotation at 255 nm or the ellipticity at 222 nm as a function of temperature. Optical rotation was measured with a Jasco Model ORD/UV-5 optical Rotation dispersion recorder with a 1-cm path length jacketed cell (Helma Cells, Jamaica, NY). Optical rotation measurements were made at 255 nm in those buffers that absorbed strongly at 222 nm. Ellipticities at 222 nm were measured in a 0.1-cm path length jacketed cell with a Cary 60 spectropolar equipped with an Aviv 100DK circular dichroism attachment obtained from Aviv Associates, Lakewood, NJ. The temperature was monitored with a subminiature thermocouple probe (Omega Engineering, Inc., Catalog no. SCPSS-020G-6) inserted through the cell stopper directly into the sample cuvette but out of the light path. The output of the thermocouple was amplified and linearized by using an Omega TAC-386-T amplifier and applied directly to the x axis input of an X–Y recorder. The output of the Cary 60 spectropolarimeter was applied to the y axis to allow direct continuous recording of the melting profiles. A heating rate of 0.3–0.5 °C min^{-1} was used to assure thermal equilibrium of the sample. Base-line drift was monitored every 10 °C by holding the temperature and recording the signal at 250 nm as a reference point. The thermal equilibrium of the sample was checked by comparing the signal at 222 nm before and after the reading at 250 nm. Some melting curves were recorded by monitoring the signal at a series of discrete temperature settings to test for thermal equilibrium. The temperature was controlled with a Brinkmann Lauda RM3 Model S-1 water bath. Rod samples were dialyzed into each buffer, diluted with dialysate, and degassed just before use. The oxidation state of the rod was determined by running SDS gels of IAA-treated samples under both reducing and nonreducing conditions to confirm that the samples were in the reduced state under various conditions. Melting curves shown below were taken with the fully reduced rod. Reduced tropomyosin (Lehrer & Morris, 1982) was kindly supplied by Dr. S. Lehrer.

Analysis of Melting Profiles. Thermodynamic parameters were obtained from melting profiles by fitting optical rotation or ellipticity data as a function of temperature according to the following analysis. Consider a CD melting curve arising from the melting of a molecule having two helical domains. In what follows, a domain is considered to be a region of the molecule which obeys two-state behavior on melting. In the case of a protein having two such helical domains, four species must be considered according to the scheme:

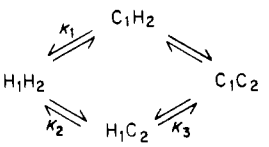

(1)

where H_i and C_i refer to helical and coiled forms of domain i.

The temperature-dependent equilibrium behavior of this system can be represented with three equilibrium constants, K_1, K_2, and K_3, according to the equation (Freire & Biltonen, 1978; Filimonov et al., 1982):

$$\theta_T = \theta_{HH}/Q + \theta_{CH}K_1/Q + \theta_{HC}K_2/Q + \theta_{CC}K_2K_3/Q \quad (2)$$

where θ_T is the total observed ellipticity at temperature T, θ_{HH}, θ_{CH}, θ_{HC}, and θ_{CC} represent the molar ellipticity of each species, and Q is the partition function given by

$$Q = 1 + K_1 + K_2 + K_2K_3$$

Each of the constants, K_i, has a temperature dependence given by eq 3 if one makes the approximation that the heat capacity change for the melting process is zero over the temperature range of the transition:

$$\ln K_i = -\Delta H^\circ_i/RT + \Delta S^\circ_i \quad (3)$$

where R is the gas constant, T is the absolute temperature, and ΔH°_i and ΔS°_i are the change in standard enthalpy and

[1] Abbreviations: IAA, iodoacetic acid; HMM, heavy meromyosin; EDTA, ethylenediaminetetraacetic acid; SDS, sodium dodecyl sulfate; S-2, subfragment 2; LMM, light meromyosin; Tris, tris(hydroxymethyl)aminomethane; BAEE, benzoyl-L-arginine ethyl ester; CD, circular dichroism; DTT, dithiothreitol.

entropy, respectively, between the various states.

There exists a temperature, $T_{m,i}$, usually referred to as the "transition temperature", at which $\Delta G°_i = 0$, defined by

$$T_{m,i} = \Delta H°_i / \Delta S°_i \quad (4)$$

which corresponds to the temperature at which the two states under consideration are equally populated. If eq 4 is substituted into eq 3, we have

$$\ln K_i = \Delta H°_i (1/T_{m,i} - 1/T)/R \quad (5)$$

In the pretransition temperature regions, a linear temperature dependence of the ellipticity has been observed (Warashina & Ikegami, 1972; Burke, et al., 1973; Hvidt et al., 1984) and was taken into account by assuming it was proportional to the number of helical residues composing each species such that

$$\theta_i = \theta_{i,20} + (\theta_{i,20} - \theta_{CC})b(T - 293.15) \quad (6)$$

where $\theta_{i,20}$ is the molar ellipticity at 20 °C (i = HH, CH, or HC), θ_{CC} is the molar ellipticity of the fully melted species, and b is the temperature coefficient. The value of θ_{CC} was assumed to be independent of temperature.

For n independently melting domains, eq 2 can be expanded and rearranged to give

$$\theta_T = \theta_n + \sum_{i=1}^{n} \Delta\theta_i/(1 + K_i) \quad (7)$$

where $\Delta\theta_i$ is the change in ellipticity upon melting of domain i and θ_n is the final ellipticity value.

The melting curves were fitted as a function of temperature to eq 2 (or 7), 5, and 6 by minimizing the sums of the squares of the deviations between the observed and calculated values with respect to the various parameters using a modified version of the simplex-directed search method as described originally by Nelder & Mead (1965). A computer program was written in Fortran-77 to perform the fits. Each parameter was allowed either to vary or to be held constant at any stage in the fitting procedure. Errors given for the parameters are the approximate 95% confidence limits calculated from the curvature of the variance hypersurface at the minimum with the assumption that the parameters are uncorrelated. Examination of isovariance plots showed that the $T_{m,i}$ were nearly orthogonal to each other and to the $\Delta H°_i$ near the minimum.

Three models were considered. In the first model, possible cooperatively between domains was taken into account by allowing all three equilibrium constants to vary independently. In the second model, the two domains were assumed to melt independently by forcing K_1 to be equal to K_3. In both models, $\theta_{HH} - \theta_{CH}$ was forced to be equal to $\theta_{HC} - \theta_{CC}$. In the third model, three independent domains were considered according to eq 7. For the first and third models, the ellipticity could be fitted as a function of temperature with 11 parameters, and the second model fitted with 8 parameters, to obtain $\Delta H°_i$ and $T_{m,i}$ in addition to the other parameters. For the first model, the values of $\Delta H°_i$ for the first, second, and third transitions were typically 220 ± 8, 60 ± 9, and 230 ± 8 kcal K^{-1} mol^{-1}, respectively. The values for $T_{m,i}$ under various conditions are given below. The values of $\Delta H°_i$ and $T_{m,i}$ for the first and third transitions were the same within experimental error; therefore, the model consisting of two independent transitions was used to obtain transition temperatures. The model comprising three independent transitions did not result in any improvements in the fits, indicating that the curves were probably not composed of more than two transitions. The standard deviation of the fits was typically in the range of 0.25–0.45% of the total change in ellipticity from 20 to 70 °C.

Table I: Kinetics of Papain Cleavage of Myosin Rod

	rate constant for disappearance of rod (min^{-1})	
molarity	sodium chloride	sodium acetate
0.6	0.056 ± 0.006	0.024 ± 0.002
1.0	0.085 ± 0.005	0.024 ± 0.002
1.5	0.240 ± 0.003	0.030 ± 0.003
2.0	0.557 ± 0.005	0.033 ± 0.004

The possibility of chain dissociation was treated by comparing melting curves obtained over a wide range of protein concentraton. A melting curve obtained at 0.5 g/L was fit to a model that included chain dissociation. The thermodynamic parameters obtained in that fit were then used to generate the melting profiles expected at other protein concentrations.

The following model, in which melting of the last domain is combined with chain dissociation in a concerted step, was used:

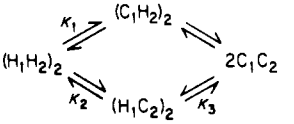

The equation describing this system is

$$C_t = [HH] + K_1[HH] + K_2[HH] + \tfrac{1}{2}(K_2K_3[HH])^{1/2}$$

where C_t is the total molar concentration of myosin rod at the start of the melting process, [HH] is the molar concentration of the fully helical species, and K_i is defined by the above scheme. The temperature dependence of K_i is given by eq 3.

The total contribution to the ellipticity at 222 nm is

$$\theta_T = \{\theta_{HH}[HH] + \theta_{CH}K_1[HH] + \theta_{HC}K_2[HH] + \theta_{CC}(K_2K_3[HH])^{1/2}\}/C_t$$

These relations were used both for curve fitting and for simulation with C_t specified as a known parameter.

Analytical Ultracentrifugation. Sedimentation velocity runs were performed on a Beckman Instruments Model E analytical ultracentrifuge equipped with a UV photoelectric scanner. Sedimentation coefficients were plotted according to

$$1/s_{20,w} = 1/s^0_{20,w}(1 + K_c c)$$

where c is the protein concentration in units of grams per liter. The values of $s^0_{20,w}$ and K_c were estimated by least squares.

Sedimentation equilibrium runs were performed as described previously (Yphantis, 1964; Margossian & Stafford, 1982).

Results

Papain Digestion of Myosin Rod. Under all solvent conditions used, papain-catalyzed hydrolysis of myosin rod resulted in the formation of LMM (M_r 75 000) and long S-2 (M_r 53 000) with appreciable amounts of short S-2 (M_r 35 000) formed at longer digestion times. However, both the kinetics and pathway of hydrolysis depended on which anion was present.

Digestions were performed at different concentrations of sodium chloride and sodium acetate (Figure 1), and rates of hydrolysis at the S-2/LMM junction were compared (Table I). The rate in chloride was strongly dependent on salt concentration while the rate in acetate was virtually unaffected. A least-squares fit of the data listed in Table I to the equation (von Hippel & Schleich, 1969):

$$\ln k = \ln k_0 + K_s[Cl^{-1}]$$

gave values for k_0 and K_s of 0.018 ± 0.003 min^{-1} and 1.68 ±

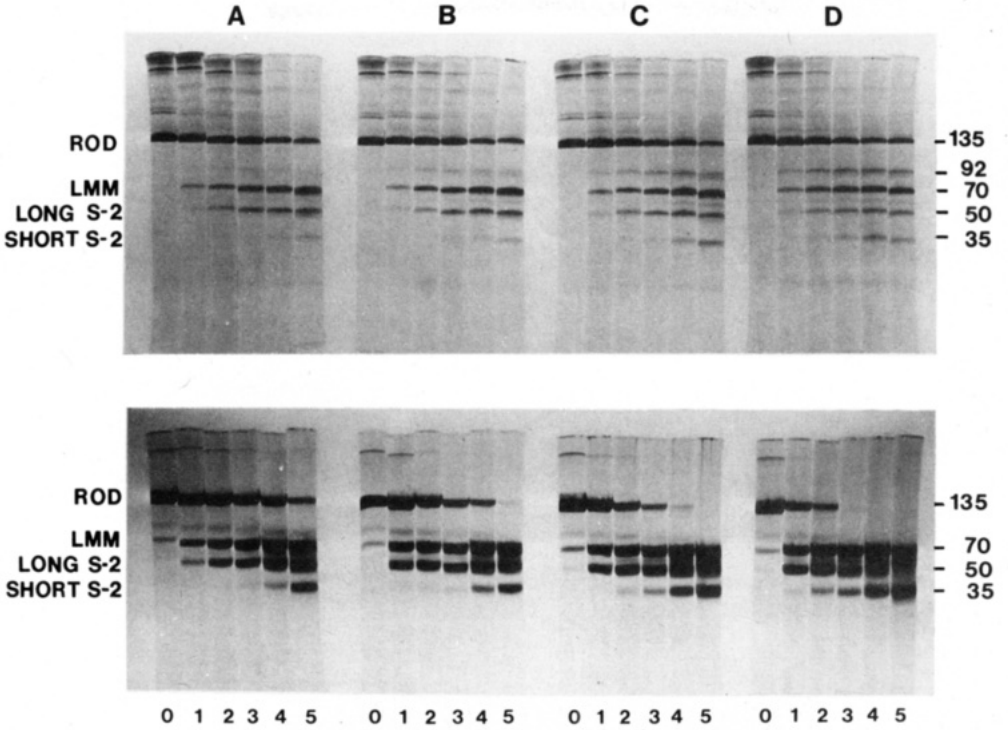

FIGURE 1: Papain digestion of rabbit myosin rod. Time series showing the effect of acetate (top) and chloride (bottom) concentration on the rate of digestion at the S-2/LMM junction. Tris–acetate/Tris–dodecyl sulfate (5%)–polyacrylamide gels: (A) 0.6 M; (B) 1.0 M; (C) 1.5 M; (D) 2.0 M. The numbers under the gels refer to the time of digestion: 0, 3, 7, 15, 30, and 60 min, respectively. The gels were densitometered, and the areas under the peaks were computed, normalized, and plotted on semilog paper. The rate constants for the disappearance of rod were computed by a least-squares fit of the logarithm of the areas vs. time. With the exception of the value for rod, the values of molecular weight are those of the known molecular weights (Margossian et al., 1981). The value of M_r 135 000 for the rod is an apparent value which is typical for rod on SDS gels.

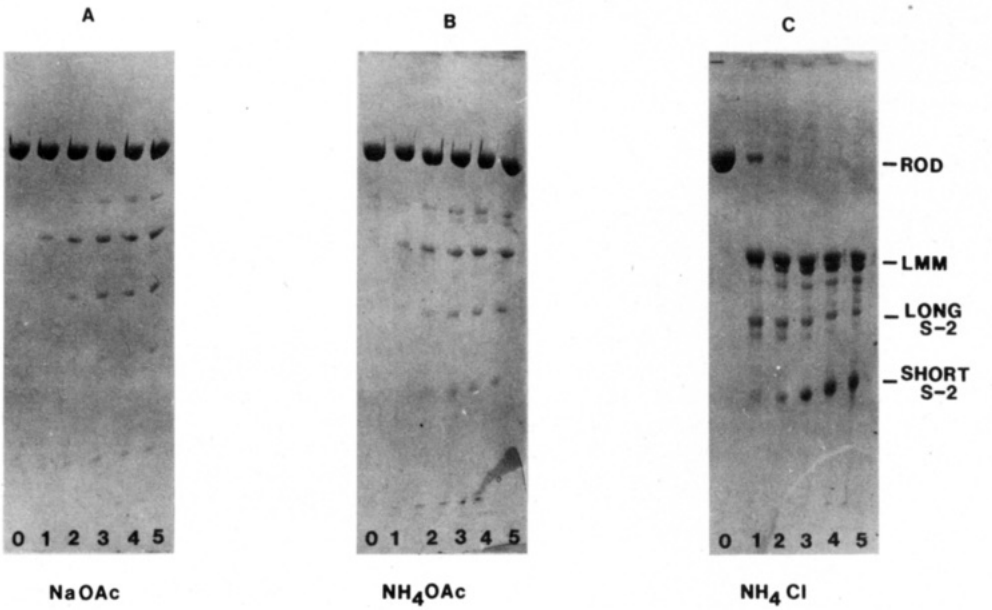

FIGURE 2: Papain digestion of rabbit myosin rod. Time series showing that changing the cation from sodium to ammonium had no significant effect on the digestion kinetics and that changing the anion from acetate to chloride accelerated the rate of digestion. All samples contained 5 mM Tris and 1 mM EDTA, pH 7.3, in addition to the salt. Microslab SDS gels (8%). Times are 0, 3, 7, 15, 30, and 60 min, corresponding to slots 0, 1, 2, 3, 4, and 5, respectively, for each set of conditions: (A) 2.0 M sodium acetate; (B) 2.0 M ammonium acetate; (C) 2.0 M ammonium chloride.

0.14 L mol^{-1}, respectively, at a papain concentration of 5.3 μm/mL and a rod concentration of 0.5 mg/mL for the kinetics of the disappearance of the rod. In acetate, values of k_0 and K_s were 0.020 ± 0.002 min^{-1} and 0.25 ± 0.05 L mol^{-1}, respectively. Substitution of sodium by ammonium ion (Figure 2) made no significant difference in the results. In either case, it was observed that hydrolysis was considerably faster in the presence of chloride than in the presence of acetate. These observations suggested that chloride ion was exerting a direct effect on the structure of the coiled-coil in the S-2/LMM junction.

The pathway as well as the rate of digestion depended on which anions were present. In either 0.6 M chloride or acetate, LMM and long S-2 were formed directly from myosin rod (pathway A in Figure 3). At higher concentrations of acetate, a second pathway (B) seemed to be operating in parallel to

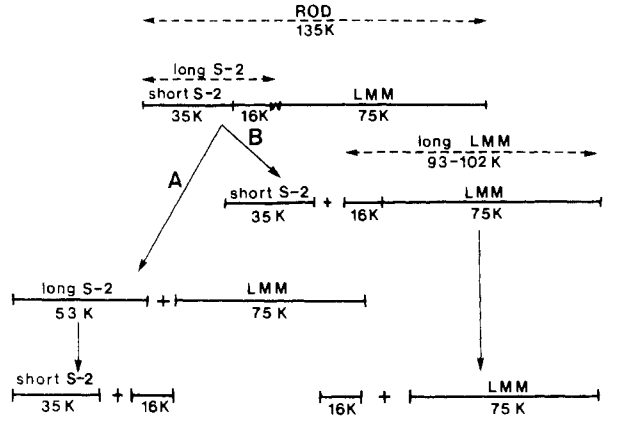

FIGURE 3: Papain digestion pathways; see text for an explanation.

pathway A. In pathway B, a pair of intermediates with a chain weight of about 102 000 and 93 000 daltons (long LMM) was formed and most likely arose by removal of short S-2 (M_r 35 000) from the N-terminal end of the rod. (Some of the material at 93 000 daltons is probably S-1 formed from a small amount of contaminating myosin.) Further cleavage of this intermediate led to the formation of LMM (M_r 75 000) and presumably a piece with a chain weight of 16 000 which was not seen on gels. In the presence of chloride, stable long LMM intermediates were not detectable. There was some indication of a series of species somewhat smaller than long LMM under these conditions (Figure 1); however, they were not always observed (Figure 2). There were some other differences in the course of digestion depending on the anion employed. In the presence of chloride ion, both LMM and long S-2 became split into doublets with the lower band having a chain weight about 3000 daltons less than the main band (Figures 1 and 2). This splitting was not observed in the absence of chloride, providing further support for the idea that chloride ion destabilizes parts of the coiled coil. Short S-2 did not form a doublet under any conditions.

Thermal Stability of Myosin Rod. The transition temperatures of CD and optical rotation melting profiles of myosin rod depended on both the nature and concentration of anions present. In either 0.6 M sodium chloride or 0.6 M ammonium chloride, a biphasic melting profile with transition temperatures at 44.8 ± 0.6 and 53.3 ± 1.6 °C, respectively, was observed, while in 0.6 M sodium or ammonium acetate, transition temperature occurred at 49.9 ± 0.6 and 58.1 ± 1.7 °C, respectively (Figures 4 and 5). Whether or not the rod had been subjected to ethanol precipitation or had been stored in 50% glycerol at −24 °C made no difference in the melting profiles; they were superimposible on those shown in Figure 5.

Dissociation of the rod was not observed over the temperature range (20–70 °C) of these experiments. The possibility of chain dissociation was investigated by performing melting curves over a wide range of protein concentration. The experimental curves did not show the concentration dependence expected for a system in which dissociation occurs (Figure 4B), indicating strongly that chain dissociation did not occur in this system. The dotted curves are experimentally obtained curves at 4.6×10^{-6} and 4.6×10^{-9} M rod concentration in 0.6 M NaCl, 5 mM phosphate, 0.1 mM EDTA, and 0.5 mM DTT, pH 7.3. The solid curve passing through the experimental points is the fit of the chain dissociation model to the experimental curve obtained at 4.6×10^{-6} M. The second solid curve is a simulated curve generated by using the values of ΔH_i and ΔS_i obtained from the fitted curve and a value of 4.6×10^{-9} M for C_t. As a control, the same type of experiment

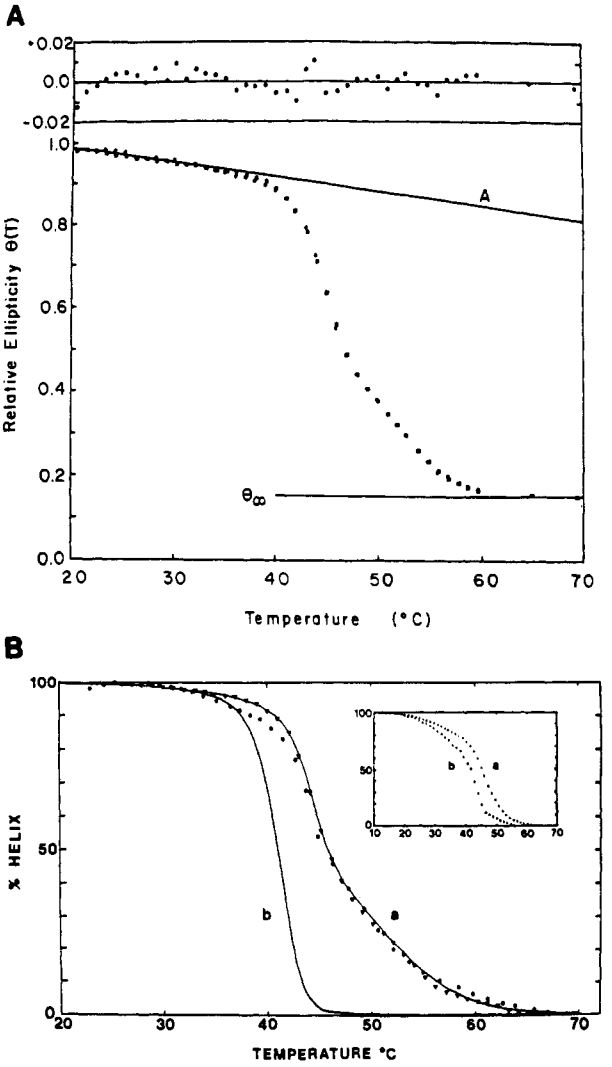

FIGURE 4: (A) Circular dichroism melting profile of myosin rod in 0.6 M NaCl, 5 mM phosphate, 0.1 mM EDTA, and 0.5 mM DTT, pH 7.3. Circles are the experimental data. Squares are the best fit using the method described in the text. Line A shows the fitted temperature dependence of the ellipticity in the pretransition region. The line labeled θ_∞ is the fitted value of the residual ellipticity at the end of the melting process. The inset at the top is a graph of the residuals of the fit on an expanded scale. Usually, better fits than this were obtained. Some of the fits were obtained from data taken every 0.2 °C over the range from 20 to 70 °C. In no case was there any indication from the distribution of residuals that more than two transitions were required to fit the data. (B) Concentration dependence of melting profiles. Melting curves of myosin rod taken at 1.0 g/L (triangles) and 0.001 g/L (circles). The solid curve (a) passing through the data is the fit obtained at 1.0 g/L with the assumption that the chains dissociate (see text). The solid curve (b) to the left of the data is a theoretical curve generated for 0.001 g/L by using the parameters obtained from the fit at 1.0 g/L. Inset: Melting curves of reduced tropmyosin obtained at (a) 1.0 and (b) 0.004 g/L in the same NaCl buffer as the rod, showing the expected concentration dependence for a system in which chain dissociation has been demonstrated (Holtzer et al., 1984). The y axis is the percent of the change in the CD signal at 222 nm. The x axis is in degrees celcius. Only every fifth point is plotted.

was carried out with tropmyosin and showed the expected concentration dependence (Figure 4B, inset) (Holtzer et al., 1983).

Thermal stability of the rod increased markedly with increasing sodium acetate concentration. Transition temperatures of optical rotation melting profiles were estimated graphically and were plotted vs. sodium acetate concentration (Figure 6, inset, solid circles). At 1.5 M acetate and above,

Table II: Dependence of Melting Transition Temperatures on Concentration of NaCl and Sodium Acetate

in 0.6 M NaCl			in 0.6 M sodium acetate		
[sodium acetate] (M)	$T_{m,1}$ (°C)	$T_{m,2}$ (°C)	[NaCl] (M)	$T_{m,1}$ (°C)	$T_{m,2}$ (°C)
0.0	44.8	53.3	0.0	49.8	58.2
0.2	47.6	56.5			
0.4	49.9	58.4	0.4	51.8	60.8
0.6[a]	52.3	62.2	0.6[a]	52.3	62.2
$K_{Ac,i}$[b]	12.4 ± 0.4	14.3 ± 1.2	$K_{Cl,i}$	4.3 ± 0.6	6.6 ± 0.1
$T^0_{m,i,Ac}$[c]	42.3	49.3	$T^0_{m,i,Cl}$	42.5	49.6

[a] Same experiment. [b] Units are °C L mol^{-1}. [c] Obtained by combining values of K_s with data in the first row using eq 8a,b. Units are degrees centigrade.

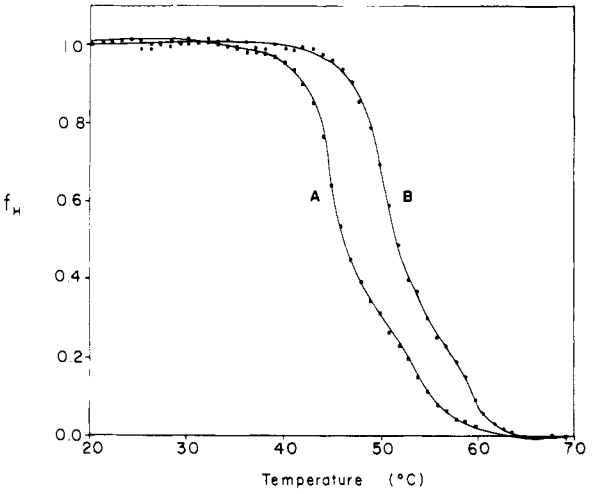

FIGURE 5: Effect of changing salt from (A) 0.6 M NaCl to (B) 0.6 M sodium acetate. Graph of the fraction of helix, f_H, which melts by 80 °C as a function of temperature. The fraction of helix at each temperature was computed by using the parameters obtained from the fitting procedure. The set of points labeled A was obtained from the data shown in Figure 4.

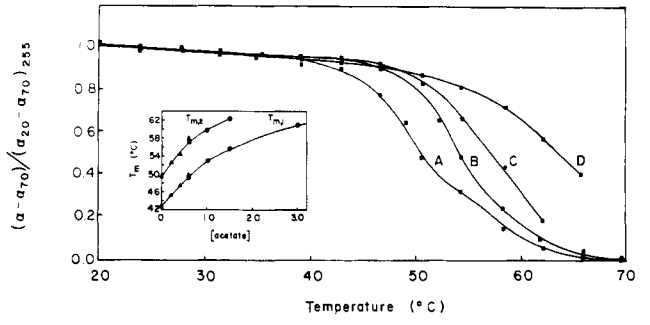

FIGURE 6: Optical rotation melting curves of myosin rod at various concentrations of sodium acetate: (A) 0.6 M; (B) 1.0 M; (C) 1.5 M; (D) 3.0 M. Inset: Graph of the transition temperatures vs. acetate concentration. Circles correspond to the curves A–D. Triangles are the values calculated from experimental data listed in Table II (see text).

the rod precipitated at the higher temperatures precluding complete melting profiles.

The effect of changing chloride concentration on melting profiles was complex and was investigated by several approaches. In the first set of experiments, at 1.0 M NaCl and above, profiles were measured at increasing total salt concentration (Figure 7). Above 1.0 M, melting curves became triphasic by 2 M with a new transition occurring at about 44 °C, shifting to 38 °C in 3.0 M NaCl and 30 °C in 4.0 M NaCl.

Below 0.6 M NaCl, two sets of experiments were performed to obtain the salt concentration dependence. In one set, acetate concentration was held at 0.6 M while NaCl concentraton was varied between 0.0 and 0.6 M, and in the other, NaCl concentration was held at 0.6 M while acetate concentration was varied between 0.0 and 0.6 M (Table II). The curves were similar to those shown in Figures 4 and 5 and are not shown. From the concentration dependence of the profiles, an estimate of $K_{Ac,i}$ and $K_{Cl,i}$ (eq 8a,b) was obtained where $i = 1, 2, ...,$

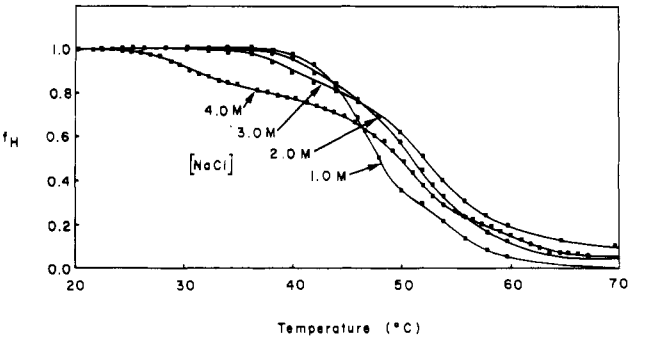

FIGURE 7: Circular dichroic melting profiles obtained at various concentrations of NaCl. The fraction of helix was calculated by using the value of the temperature dependence in the pretransition region obtained in 0.6 M NaCl. Since these curves exhibited more than two transitions, they were not analyzed with the curve-fitting program. See text for further explanation.

$$T_{m,i} = T_{m,i}^0 + K_{Ac,i}[Ac^{-1}] \quad (8a)$$

$$T_{m,i} = T_{m,i}^0 + K_{Cl,i}[Cl^{-1}] \quad (8b)$$

etc. and refers to the transition, $T_{m,i}$ is the transition temperature of the ith transition, $T_{m,i}^0$ is the value of $T_{m,i}$ at $c = 0$, and $K_{Ac,i}$ and $K_{Cl,i}$ are coefficients reflecting the dependence of each transition temperature on the concentration of acetate and chloride, respectively. Values of 12.4 ± 0.4 and 14.3 ± 1.2 °C L mol^{-1} for $K_{Ac,1}$ and $K_{Ac,2}$, respectively, were found The dependence on NaCl concentration was found to be smaller than for acetate, giving 4.3 ± 0.6 and 6.6 ± 0.1 °C L mol^{-1} for $K_{Cl,1}$ and $K_{Cl,2}$, respectively. The $T_{m,i}$ data for acetate are plotted in the inset of Figure 6 (solid triangles) after subtraction of the contribution from 0.6 M NaCl.

The dependence of the thermal stability of the rod was not significantly dependent on ionic strength. Experiments were carried out to determine whether the concentration dependence of melting profiles could be attributed to changes in ionic strength or to effects either on the structure of myosin or on the structure of the solvent. To study the effect of varying salt concentration at constant ionic strength, melting profiles were measured in mixtures of NaCl and sodium acetate at a total salt concentration of 0.6 M. The melting curves (not shown) fell between those for 0.6 M acetate and 0.6 M chloride alone (Table III). These experiments showed that variations in salt concentration caused an effect independent of any ionic strength effect. To rule out an ionic strength effect, the results at constant ionic strength were compared to those obtained at variable ionic strength. Variation of ionic strength was shown to have a negligible effect by using the results obtained

Table III: Dependence of Transition Temperatures on Salt Concentration at Constant Ionic Strength

[NaCl] (M)	[sodium acetate] (M)	$T_{m,1}$ (°C)	$T_{m,2}$ (°C)	$T_{m,1calcd}$[a] (°C)	$T_{m,2calcd}$[a] (°C)
0.00	0.60	49.8 ± 0.6	58.2 ± 1.7	50.3	58.0
0.12	0.48	48.8 ± 0.3	57.0 ± 0.9	49.4	57.0
0.24	0.36	47.2 ± 0.3	54.9 ± 0.7	48.4	56.1
0.36	0.24	46.7 ± 0.4	55.1 ± 1.1	47.4	55.2
0.48	0.12	45.4 ± 0.4	53.3 ± 1.1	46.4	54.3
0.60	0.00	44.8 ± 0.6	53.3 ± 1.6	45.5	53.4

[a] Calculated by using eq 9.

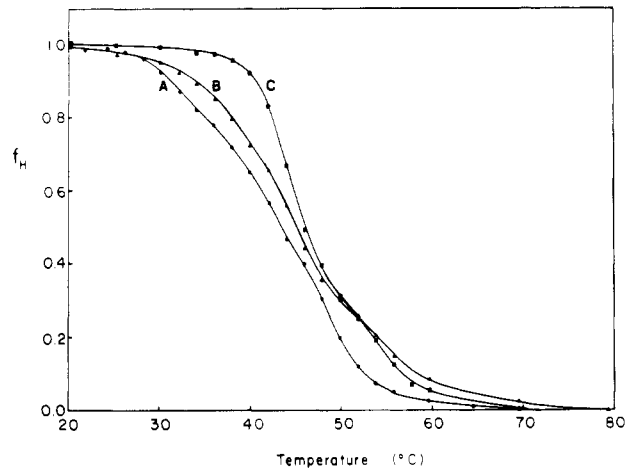

FIGURE 8: Circular dichroic melting profiles obtained in (A) 2 mM pyrophosphate, pH 9.3, (B) 0.6 M KCl and 10 mM pyrophosphate, pH 9.5, and (C) 0.6 M KCl and 10 mM pyrophosphate, pH 7.3.

above for the $T_{m,i}^0$ values and $K_{Cl,i}$ at 0.6 M acetate and $K_{Ac,i}$ at 0.6 M NaCl to calculate values of $T_{m,i}$ that would have been expected for the constant ionic strength mixtures using the assumption that effects of acetate and chloride were additive (von Hippel & Schleich, 1969) according to the following relationship:

$$T_{m,i} = T_{m,i}^0 + K_{Ac,i}[Ac^{-1}] + K_{Cl,i}[Cl^{-1}] \quad (9)$$

When calculated values were compared to observed values, the agreement was good with no systematic deviations outside experimental error (Table III), indicating that electrostatic interactions are probably not important to the stability of myosin rod over the range of salt concentrations studied. If ionic strength had been a significant factor, calculated values would not have agreed with observed ones.

At high pH and low ionic strength (2 mM pyrophosphate at pH 9.3), the melting profile became triphasic (Figure 8). Two of the transitions, at least 42 and 49 °C, probably correspond to the ones seen in NaCl. Whether or not the third transition, at about 33 °C, corresponded to the new one seen in 3 M NaCl was not determined. A broad profile was seen also in 0.6 M KCl, and 10 mM pyrophosphate, pH 9.5, although the third transition was not as pronounced as at the lower ionic strength. In 0.6 M KCl and 10 mM pyrophosphate, pH 7.3, the profile was essentially the same as that observed in 0.6 M NaCl, 5 mM phosphate, and 0.1 mM EDTA, pH 7.3.

Effect of Other Anions. Melting transitions in the presence of anions other than chloride and acetate were observed by following optical rotation at 255 nm. Nitrate (0.6 M) gave a curve similar to that of 0.6 M chloride (Figure 9) while the ionic forms of several carboxylic acids, namely, propionate, glutamate, and glycinate, gave curves similar to that of acetate.

Sedimentation Behavior of Rod. Sedimentation analysis revealed a single sharp boundary in both 0.6 M NaCl and 0.6 M sodium acetate (5 mM phosphate and 0.1 mM EDTA, pH 7.3). In 0.6 M NaCl, values of $s^0_{20_w}$ of 3.91 ± 0.03 S and K_c of 0.30 ± 0.03 L/g were obtained over a concentration range of 0.15–0.56 g/L. In 0.6 M sodium acetate, values of 3.88 ± 0.03 S and 0.29 ± 0.02 L/g, respectively, were obtained, indicating that sedimentation behavior of the rod did not depend upon whether chloride or acetate was present.

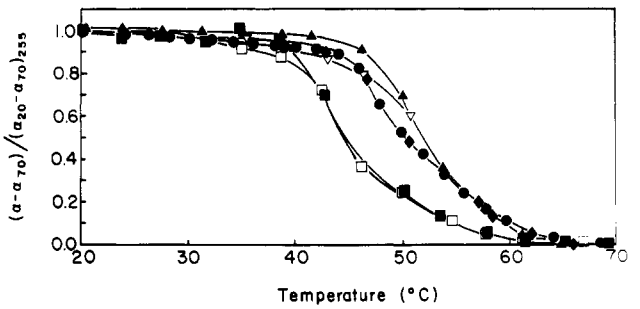

FIGURE 9: Optical rotation melting profiles obtained in (closed squares) 0.6 M $NaNO_3$, (closed triangles) 0.6 M propionate, (open, inverted triangles) 0.6 M glutamate, (closed circles) 0.6 M glycine, (open squares) 0.6 M NaCl, and (closed diamonds) 0.6 M sodium acetate (all in 5.0 mM phosphate and 0.1 mM EDTA, pH 7.3).

Molecular weight measurements were carried out by equilibrium ultracentrifugation in both sodium chloride and sodium acetate (0.6 M) containing buffers. The same value of 220 000 for molecular weight was obtained in each buffer, showing that the rod did not aggregate in the presence of either salt.

Discussion

Chloride ion has a tendency to destabilize the structure of the myosin coiled coil in or near the S-2/LMM junction. This conclusion was drawn both from digestion experiments in which the rate of papain digestion at the S-2/LMM junction increased with increasing chloride ion concentration and from thermal melting experiments in which it was observed that chloride destabilized a portion of the coiled coil. Two melting transitions were observed at moderate concentrations (0.6 M) of all anions used. In the presence of acetate, increasing the salt concentration resulted in an increase in thermal stability of the entire rod. However, in the presence of chloride, at the highest concentrations a new melting transition was observed whose stability decreased with increasing chloride concentration (Figure 7). At the same high concentrations of acetate, no new transitions were observed. These results suggest that chloride binds directly in or near the S-2/LMM junction and may increase its flexibility at salt concentrations used commonly to study myosin in solution. At high pH and low ionic strength, the rod exhibited broad melting profiles, indicating that portions of the rod were less stable and possibly more flexible than at neutral pH (Figure 8).

Others have seen more than two thermal transitions in myosin rod by differential scanning calorimetry. Potekhin et al. (1979) have observed a melting profile showing three major peaks which they were able to resolve into six apparent transitions using a deconvolution method described by Freire & Boltonin (1978). The three major transitions may correspond to the three seen in this study at high chloride con-

centrations. However, a more likely explanation for their observation of more than two transitions is that some of the heat absorbed may have gone into other independent processes that are not accompanied by a significant disruption of the secondary structure. The good fits of the data to eq 2 suggest that only two of the six processes observed by Potehkin et al. (1979) were accompanied by significant changes in the helical secondary structure reflected in the CD signal at 222 nm. The enthalpy change obtained by curve fitting for the first transition was about 200 kcal/mol, in agreement with their value of 196 kcal/mol [cf. Privalov (1982)]. The enthalpy change obtained for the second process was about 60 kcal/mol and does not correspond to any of the other values reported by Privalov (1982).

Many studies of myosin and other muscle proteins are carried out in the presence of chloride ions at concentrations in a range (0.05–0.6 M) considerably higher than in vivo levels (see references cited above). The results presented here as well as others reported (Magid & Reedy, 1980; Crowther et al., 1985) suggest that the choice of supporting electrolyte, particularly chloride, may influence the results of in vitro experiments involving myosin.

ACKNOWLEDGMENTS

I thank Drs. J. Gergely and S. Lehrer for thought-provoking discussions and critical comments. I also thank Dr. S. Hvidt for stimulating discussions and D. Lapenta, P. Sarkar, and C. Monks for their excellent technical assistance.

Registry No. Chloride, 16887-00-6; acetate ion, 71-50-1; papain, 9001-73-4; nitrate ion, 14797-55-8; propionate ion, 72-03-7; glutamate ion, 11070-68-1; glycinate ion, 23297-34-9.

REFERENCES

Adrian, R. H. (1961) *J. Physiol. (London) 156*, 623–632.
Bolton, T. B., & Vaughan-Jones, R. D. (1977) *J. Physiol. (London) 270*, 801–833.
Brahms, J., & Brezner, J. (1961) *Arch. Biochem. Biophys. 95*, 219.
Burke, M., Himmelfarb, S., & Harrington, W. F. (1973) *Biochemistry 12*, 701–709.
Crowther, R. A., Padron, R., & Craig, R. (1985) *J. Mol. Biol.* (in press).
de la Torre, J. G., & Bloomfield, V. A. (1980) *Biochemistry 19*, 5118–5123.
Elliot, A., & Offer, G. (1978) *J. Mol. Biol. 123*, 505–519.
Filimonov, V. V., Potekhin, S. V., Matveev, P. L., & Privalov, P. L. (1982) *Mol. Biol. (Moscow) 16*, 551–562.
Freire, E., & Biltonen, R. L. (1978) *Biopolymers 17*, 463–479.
Harris, E. J. (1963) *J. Physiol. (London) 166*, 87–109.
Harvey, S. C., & Cheung, H. C. (1977) *Biochemistry 16*, 5181–5187.
Highsmith, S., Kretzschmar, K. M., O'Konski, C. T., & Morales, M. F. (1977) *Proc. Natl. Acad. Sci. U.S.A. 74*, 4986–4990.
Highsmith, S., Wang, C., Zero, K., Pecora, R., & Jardetzky, O. (1982) *Biochemistry 21*, 1192–1197.
Hofmeister, F. (1888) *Arch. Exp. Pathol. Pharmakol. 24*, 247–256.
Holtzer, M. E., Holtzer, A., & Skolnick, J. (1983) *Macromolecules 16*, 173.
Hvidt, S., Nestler, H. M., Greaser, M. L., & Ferry, J. D. (1982) *Biochemistry 21*, 4064.
Hvidt, S., Ferry, J. D., Roelke, D. L., & Greaser, M. L. (1983) *Macromolecules 16*, 740.
Hvidt, S., Rogers, M. E., & Harrington, W. F. (1984) *Biophys. J. 45*, 111a.
Kominz, D. R., Mitchell, E. T., Nihei, T., & Kay, C. M. (1965) *Biochemistry 4*, 2373–2382.
Lehrer, S. S., & Morris, E. P. (1982) *J. Biol. Chem. 257*, 8073.
Lowey, S., Slayter, H. S., Weeds, A. G., & Baker, H. (1969) *J. Mol. Biol. 42*, 1–29.
Macchia, D. D., & Baumgarten, C. M. (1979) *Pfluegers Arch. 382*, 193–195.
Magid, A., & Reedy, M. K. (1980) *Biophys. J. 30*, 27–40.
Margossian, S. M., & Lowey, S. (1982) *Methods Enzymol. 85B*, 55–71.
Margossian, S. M., & Stafford, W. F. (1982) *J. Biol. Chem. 257*, 1160.
Margossian, S. M., Stafford, W. F., & Lowey, S. (1981) *Biochemistry 20*, 2151–2155.
Matsudaira, P. T., & Burgess, D. R. (1978) *Anal. Biochem. 87*, 386–396.
Nelder, J. A., & Mead, R. (1965) *Comput. J. 7*, 308–313.
Potekhin, S. A., Trapkov, V. A., & Privalov, P. L. (1979) *Biofizika 24*, 46–50.
Privalov, P. L. (1982) *Adv. Protein Chem. 35*, 1–104.
Rosser, R. W., Schrag, J. L., Ferry, F. D., & Greaser, M. L. (1977) *Macromolecules 10*, 978–998.
Seidel, J. C. (1969) *J. Biol. Chem. 244*, 1142.
Stafford, W. F. (1984a) *Biophys. J. 45*, 224a.
Stafford, W. F. (1984b) *Abstracts of the 8th International Congress of Biophysics*, p 208, International Union for Pure and Applied Biophysics and The Royal Society of London.
Stafford, W. F., & Yphantis, D. A. (1972) *Biochem. Biophys. Res. Commun. 49*, 848.
Stafford, W. F., & Margossian, S. S. (1982) *Biophys. J. 37*, 55a.
Stafford, W. F., Szentkiralyi, E. M., & Szent-Gyorgyi, A. G. (1979) *Biochemistry 18*, 5273–5280.
Tonomura, Y., Sekiya, K., & Imamura, K. (1962) *J. Biol. Chem. 237*, 3110.
Von Hippel, P. H., & Schleich, T. (1969) in *Biological Macromolecules* (Timasheff, S., & Fasman, G., Eds.) Vol. II, Marcel Dekker, New York.
Warashnia, A., & Ikegami, A. (1972) *Biopolymers 11*, 529–547.
Warren, J. C., Stowring, L., & Morales, M. F. (1966) *J. Biol. Chem. 214*, 309.
Yphantis, D. A. (1964) *Biochemistry 3*, 297.